Order online now!

www.rockland.com
tech@rockland.com
+1 484.791.3823

Datasheet for 600-401-919

SMAD3 phospho S423/phospho S425 Antibody

Overview

Description:	Anti-SMAD3 pS423 pS425 (RABBIT) Antibody - 600-401-919
Item No.:	600-401-919
Size:	100 µg
Applications:	ELISA, IHC, WB, IF, IP, Multiplex
Reactivity:	Human
Host Species:	Rabbit

Product Details

Background:	This antibody is designed, produced, and validated as part of a collaboration between Rockland and the National Cancer Institute (NCI) and is suitable for Cancer, Immunology and Nuclear Signaling research. Smad3 (also known as Mothers against decapentaplegic homolog 3 Mothers against DPP homolog 3, Mad3, hMAD-3, JV15-2 or hSMAD3) is a transcriptional modulator activated by TGF-beta (transforming growth factor) and activin type 1 receptor kinase. These activators exert diverse effects on a wide array of cellular processes. The Smad proteins mediate much of the signaling responses induced by the TGF-b superfamily. Briefly, activated type I receptor phosphorylates receptor-activated Smads (R-Smads) at their c-terminal two extreme serines in the SSXS motif, e.g. Smad2 and Smad3 proteins in the TGF-b pathway, or Smad1, Smad5 or Smad8 in the BMP pathway. Then the phosphorylated R-Smad translocated into nucleus, where they regulate transcription of target genes. Based on microarray and animal model experiments, Smad3 accounts for at least 80% of all TGF-b-mediated response.
Synonyms:	rabbit anti-SMAD3 pS423pS425 antibody, SMAD-3, SMAD 3, mothers against decapentaplegic homolog 3 antibody, MAD homolog 3, Mothers against DPP homolog 3, SMAD family member 3, MADH3, MADH 3, JV15-2, nothing
Host Species:	Rabbit
Clonality:	Polyclonal
Format:	IgG

Target Details

Gene Name:	SMAD3

Reactivity:	Human
PTM Specificity:	Phosphorylation
Immunogen Type:	Conjugated Peptide
Immunogen:	Anti-SMAD3 pS423pS425 antibody was prepared from whole rabbit serum produced by repeated immunizations with a dual phosphorylated synthetic peptide corresponding to a c-terminal region with Serine 423 and Serine 425 of human SMAD3 protein.
Purity/Specificity:	This affinity-purified antibody is directed against the phosphorylated form of human Smad3 protein at the pS423 and pS425 residues. The product was affinity purified from monospecific antiserum by immunoaffinity purification. Antiserum was first purified against the phosphorylated form of the immunizing peptide. The resultant affinity purified antibody was then cross adsorbed against the non-phosphorylated form of the immunizing peptide. Reactivity occurs against human Smad3 pS423 and pS425 protein and the antibody is specific for the phosphorylated form of the protein. Reactivity with non-phosphorylated human Smad3 is minimal by ELISA and western blot. Expect reactivity against phosphorylated Smad1 and Smad5. Negligible reactivity is seen against other phosphorylated Smad family members. A BLAST analysis was used to suggest cross reactivity with Smad3 from human, Xenopus laevis, Xenopus tropicalis, zebrafish, rat, mouse, swine, bovine and chicken based on 100% sequence homology with the immunogen. Reactivity against homologues from other sources is not known.
Relevant Links:	• NCBI - 5174513 • UniProtKB - P84022 • GeneID - 4088

Application Details

Tested Applications:	ELISA, IHC, WB
Suggested Applications:	IF, IP, Multiplex (Based on references)
Application Note:	This affinity purified antibody has been tested for use in ELISA, immunohistochemistry, and western blot. Specific conditions for reactivity should be optimized by the end user. Expect a band approximately 48 kDa in size corresponding to phosphorylated Smad3 protein by western blotting in the appropriate stimulated tissue or cell lysate or extract. Less than 0.2% reactivity is observed against the non-phosphorylated form of the immunizing peptide. This antibody is phospho specific for dual phosphorylated pS423 and pS425 of Smad3. Stimulation with 2 ng/ml TGF-beta for 1 hour is suggested.
Assay Dilutions:	All assays should be optimized by the user. Recommended dilutions (if any) may be listed below.
ELISA:	1:15,000 - 1:30,000
FC:	User Optimized

IHC:	1:500
WB:	1:2,000 - 1:20,000

Formulation

Physical State:	Liquid (sterile filtered)
Concentration:	1.10 by UV absorbance at 280 nm
Buffer:	0.02 M Potassium Phosphate, 0.15 M Sodium Chloride, pH 7.2
Preservative:	0.01% (w/v) Sodium Azide
Stabilizer:	None

Shipping & Handling

Shipping Condition:	Dry Ice
Storage Condition:	Store vial at -20° C prior to opening. Aliquot contents and freeze at -20° C or below for extended storage. Avoid cycles of freezing and thawing. Centrifuge product if not completely clear after standing at room temperature. This product is stable for several weeks at 4° C as an undiluted liquid. Dilute only prior to immediate use.
Expiration:	Expiration date is one (1) year from date of receipt.

Images

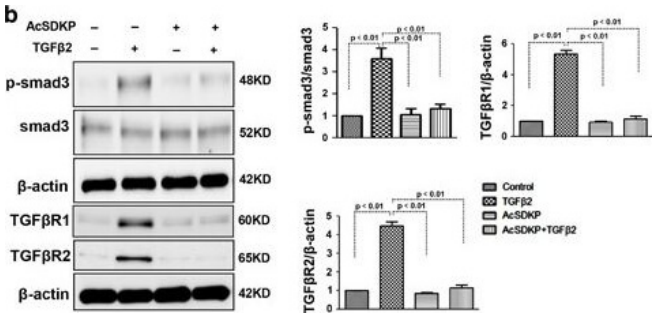

Western Blot

Proximity between AcSDKP and FGFR1 inhibits the TGFβ/smad signaling pathway in HMVECs. (a) HMVECs were treated with N-FGFR1 (1.5 μg/ml) for 48 h with or without preincubation with AcSDKP (100 nM) for 2 h, and the proximity between AcSDKP and FGFR1 was analyzed by the Duolink In Situ Assay. For each slide, images at a × 400 original magnification were obtained from six different areas. (b and c) HMVECs were treated with TGFβ2 (5 ng/ml) for 15 min or 48 h with or without preincubation with AcSDKP for 2 h, and the p-smad3, TGFβR1, TGFβR2 and FGFR1 levels were analyzed by western blot. Densitometric analysis of the p-smad3/smad3, TGFβR1/β-actin, TGFβR2/β-actin and FGFR1/β-actin levels from each group (n=6) were analyzed. (d and e) HMVECs were incubated with TGFβ2 for 15 min or 48 h with or without preincubation with AcSDKP or its mutants (AcDSPK, AcSDKA, AcADKP) (100 nM) for 2 h. The p-smad3/smad3, TGFβR1/β-actin, TGFβR2/β-actin and FGFR1/β-actin protein levels were analyzed by western blot Figure provided by CiteAb. Source: Cell Death Dis, PMID: 28771231.

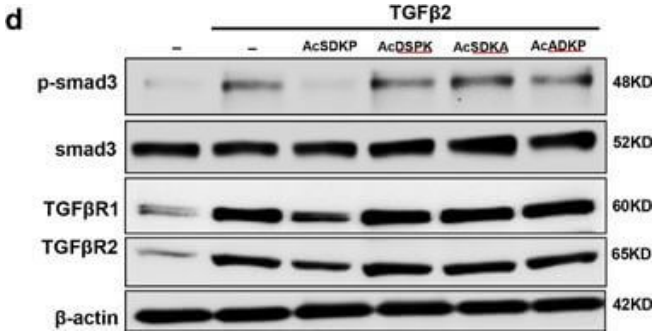

Western Blot

Proximity between AcSDKP and FGFR1 inhibits the TGFβ/smad signaling pathway in HMVECs. (a) HMVECs were treated with N-FGFR1 (1.5 μg/ml) for 48 h with or without preincubation with AcSDKP (100 nM) for 2 h, and the proximity between AcSDKP and FGFR1 was analyzed by the Duolink In Situ Assay. For each slide, images at a × 400 original magnification were obtained from six different areas. (b and c) HMVECs were treated with TGFβ2 (5 ng/ml) for 15 min or 48 h with or without preincubation with AcSDKP for 2 h, and the p-smad3, TGFβR1, TGFβR2 and FGFR1 levels were analyzed by western blot. Densitometric analysis of the p-smad3/smad3, TGFβR1/β-actin, TGFβR2/β-actin and FGFR1/β-actin levels from each group (n=6) were analyzed. (d and e) HMVECs were incubated with TGFβ2 for 15 min or 48 h with or without preincubation with AcSDKP or its mutants (AcDSPK, AcSDKA, AcADKP) (100 nM) for 2 h. The p-smad3/smad3, TGFβR1/β-actin, TGFβR2/β-actin and FGFR1/β-actin protein levels were analyzed by western blot Figure provided by CiteAb. Source: Cell Death Dis, PMID: 28771231.

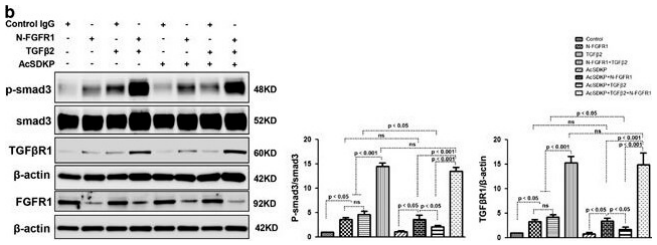

Western Blot

AcSDKP suppresses TGFβ/smad signaling and EndMT through the FGFR1/FRS2 pathway. (a) HMVECs were treated with N-FGFR1 for 48 h, and the FGFR1, TGFβR1 and TGFβR2 protein levels were analyzed by western blot. (b) HMVECs were treated with TGFβ2 in the presence or absence of N-FGFR1 for 15 min with or without AcSDKP preincubation. The p-smad3 and TGFβR1 protein levels were analyzed by western blot. Densitometric analysis of the p-smad3/smad3 and TGFβR1/β-actin levels (n=3) in each group was performed. (c) HMVECs were incubated with either N-FGFR1 in the presence or absence of TGFβ2 for 48 h with or without preincubation with AcSDKP for 2 h or with N-FGFR1 in the presence or absence of TGFβ2 for 48 h with or without 24 h of incubation with FGF2 (50 ng/ml). The CD31, SM22α, FSP1 and α-SMA protein levels were analyzed by western blot. (d) HMVECs were transfected with FRS2 siRNA (100 nM) for 48 h with or without AcSDKP preincubation. The VE-cadherin, FSP1, vimentin, SM22α and p-smad3 levels were analyzed by western blot. (e) HMVECs were treated with N-FGFR1 for 48 h or 15 min in the presence or absence of N-TGFβ (1, 2, 3) (1.0 μg/ml). The CD31, VE-cadherin, SM22α, FSP1, TGFβR1, TGFβR2 and p-smad3 levels were analyzed by western blot Figure provided by CiteAb. Source: Cell Death Dis, PMID: 28771231.

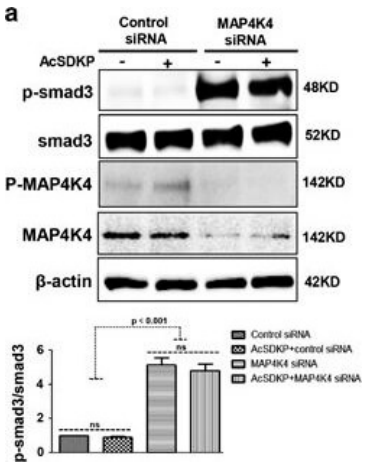

Western Blot

MAP4K4 deficiency induces TGFβ/smad signaling and EndMT via activation of integrin β1. (a) HMVECs were transfected with MAP4K4 siRNA (100 nM) for 48 h. Next, the cells were treated with or without AcSDKP for 2 h. The p-smad3/smad3 pathway was analyzed by western blot. Densitometric analysis of the p-smad3/smad3 levels was performed, with n=3 for each group. (b) HMVECs were treated with MAP4K4 siRNA for 48 h with or without AcSDKP treatment. The VE-cadherin, CD31, FSP1, SM22α and vimentin protein levels were analyzed by western blot. (c) HMVECs were transfected with MAP4K4 siRNA for 48 h in the presence or absence of TGFβ2 with or without AcSDKP. The integrin β1 level was analyzed by western blot Figure provided by CiteAb. Source: Cell Death Dis, PMID: 28771231.

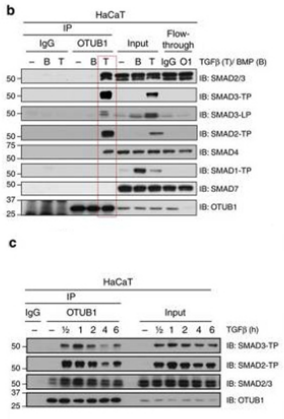

Western Blot
(b) An endogenous IP with OTUB1 antibody or pre-immune sheep IgG was performed in HaCaT cell extracts, stimulated without or with 50 pM TGFβ or 25 ng ml−1 BMP for 1 h. Cell extracts (input), endogenous IgG or OTUB1 IPs and the corresponding immune-depleted flow-through extracts (O1=OTUB1-depleted untreated HaCaT extract) were resolved by SDS-PAGE and immunoblotted (IB) with the indicated antibodies [Anti-phospho-Ser423/425 SMAD3 (SMAD3-TP; p/n 600-401-919) and anti-phospho-Thr179 SMAD3 (SMAD3-LP; p/n 600-401-C48]. (c) As in b, except that a time course of 50 pM TGFβ treatment was performed for up to 6 h before lysis. Fig 1. PMID: 24071738

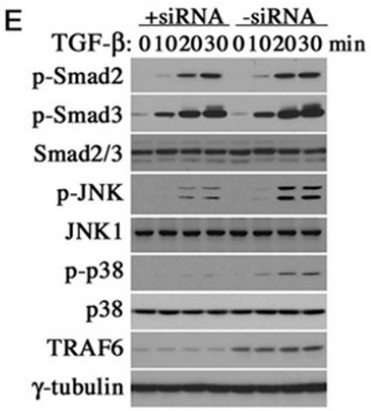

Western Blot
(E) TGF-β-induced Smad2 and Smad3 activation in AML12 cells in the presence or absence of transfected TRAF6 siRNA. (p-Smad3 p/n 600-401-919)
Fig 4. PMID: 18922473

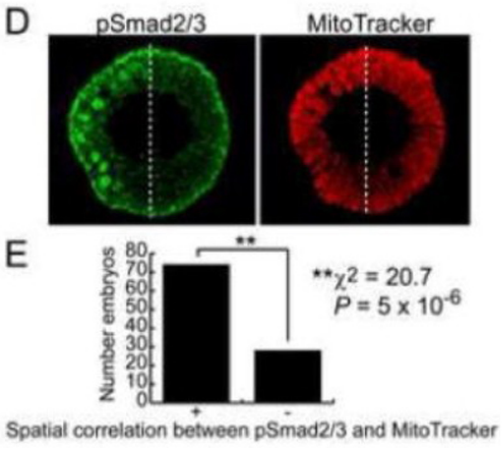

Immunofluorescence Microscopy
(D) Lateral view of an embryo stained with phospho-Smad2/3 (left) and MitoTracker (right); the dashed line (corresponding to the animal-vegetal axis) shows how the embryo image was partitioned for quantitation of MitoTracker intensity. Stained with rabbit anti-phospho-Smad3 (p/n 600-401-919). (E) Graph plotting percentage of embryos for which mean MitoTracker intensity on the half of the embryo displaying elevated phospho-Smad2/3 was either greater (+) or less (-) than that for the whole, obtained from partitioned images of embryos such as those depicted in (D). A chi-squared test with one degree of freedom (n=102) was used to test significance (**). Fig 1.
PMID: 19328778

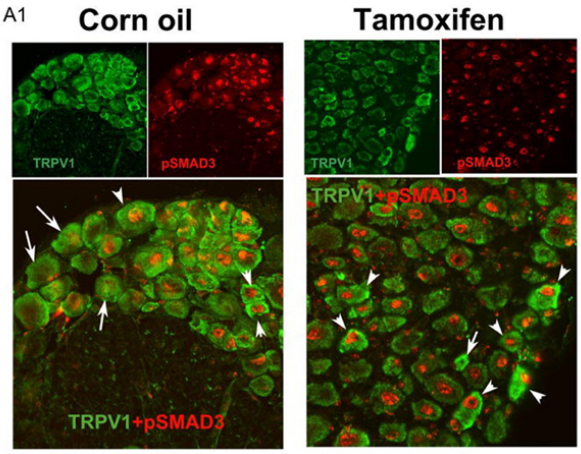

Immunofluorescence Microscopy
A) SMAD signaling in pancreatic nociceptive neurons was increased in tamoxifen-induced β1glo/Ptf1acre-ER mice. A1. An example of pSmad3 (red) and TRPV1 (green) staining in DRGT8-12 neurons of β1glo/Ptf1acre-ER mice. Arrows indicate TRPV1-positive neurons expressing pSmad3; Arrowheads indicate TRPV1-positive neurons that do not express pSmad3. Fig 2. PMID: 29505748

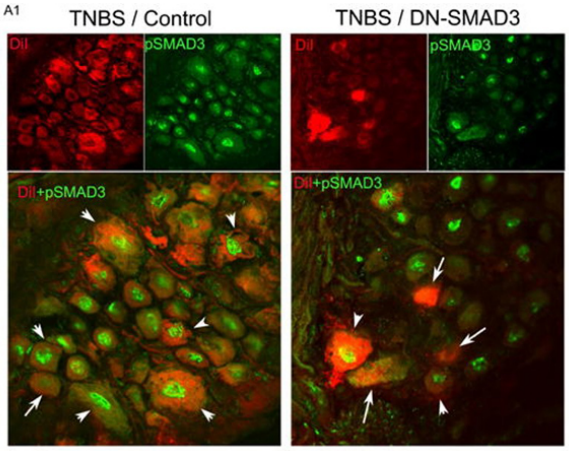

Immunofluorescence Microscopy
A): SMAD signaling in pancreatic neurons. A1: An example of pSmad3 staining (green) in Di-I labeled pancreatic neurons (red). Arrowheads indicate Di-I labeled pSmad3 positive neurons and arrows indicate Di-I labeled pSmad3 negative neurons. Fig 5. PMID: 29505748

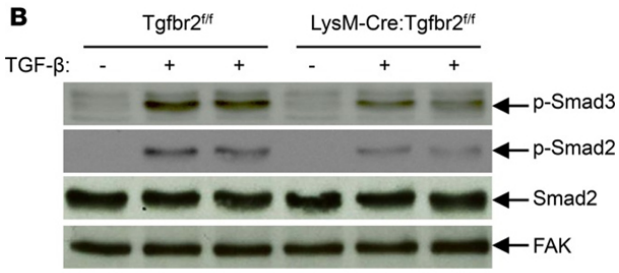

Western Blot
(B) Macrophages were stimulated with 2 ng/ml recombinant TGF-β for 30 minutes. TGF-βRII deletion led to decreases in TGF-β–stimulated phosphorylation of Smad2 and Smad3, an indication of TGF-βRII deficiency. Smad2 (p/n 600-401-A59); p-Smad3, phospho-Smad3 (p/n 600-401-919); p-Smad2, phospho-Smad2 (p/n 600-401-K09); FAK, focal adhesion kinase. Fig 1. PMID: 30385721

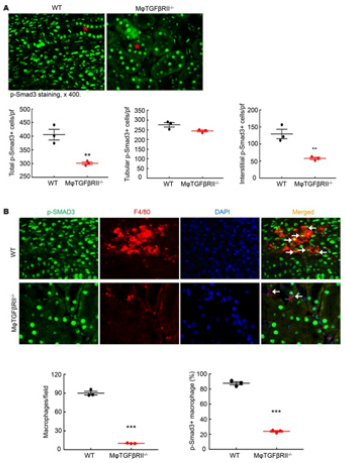

Immunofluorescence Microscopy
Mice were studied 4 weeks after severe I/R injury. (A) CD11b-Cre Tgfbr2fl/fl (macrophage TGF-βRII–/–) mice had fewer total p-Smad3-positive cells due to decreased interstitial p-Smad3-positive cells but not tubular p-Smad3-positive cells. Asterisk: tubule. **P < 0.01, n = 3 in each group. (B) p-Smad3 and F4/80 double immunofluorescent staining determined decreased renal macrophages as well as decreased macrophage TGF-β signaling in macrophage TGF-βRII–/– mice. Arrowheads: double-positive cells. ***P < 0.001, n = 3 in each group. Original magnification: ×400. Fig 7. PMID: 30385721

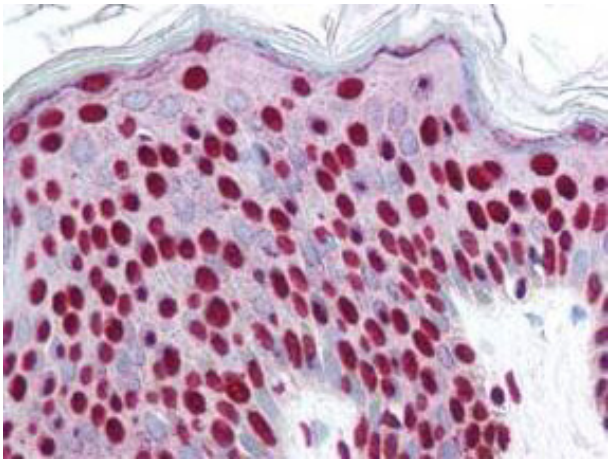

Immunohistochemistry
Rockland's affinity purified anti-Smad3 pS423 pS425 antibody was used at 2.5 ug/ml to detect signal in a variety of tissues including multi-human, multi-brain and multi-cancer slides. This image shows strong nuclear staining in the majority of epidermal keratinocytes at 40X. Tissue was formalin-fixed and paraffin embedded. The image shows localization of the antibody as the precipitated red signal, with a hematoxylin purple nuclear counterstain. Personal Communi-cation, Tina Roush, LifeSpanBiosciences, Seattle, WA.

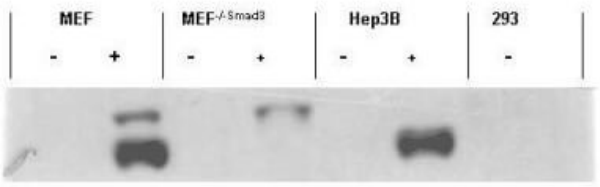

Western Blot
Western blot using Rockland's affinity purified anti-Smad3 pS423 pS425 antibody shows detection of endogenous Smad3 in stimulated cell lysates. Lysates were prepared from control cells (- lanes), or cells stimulated with 2 ng/ml TGF (+lanes) for 1 hour. This reagent recognizes phosphorylated Smad3 and has negligible reactivity against non-phosphorylated Smad3 protein. Personal Communication. Ying Zhang, NIH, CCR, Bethesda, MD.

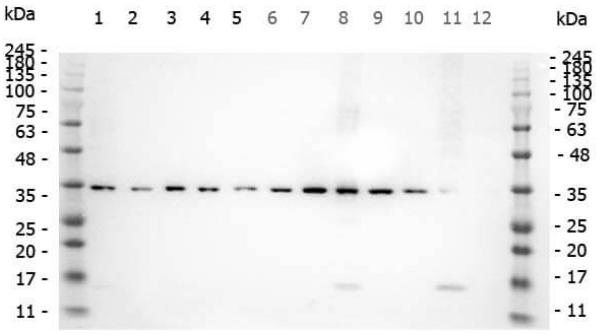

Western Blot

Western Blot of Rabbit anti-SMAD3 pS423 pS425 antibody. Marker: Opal Pre-stained ladder (p/n MB-210-0500). Lane 1: HEK293 lysate (p/n W09-000-365). Lane 2: HeLa Lysate (p/n W09-000-364). Lane 3: MCF-7 Lysate (p/n W09-000-360). Lane 4: Jurkat Lysate (p/n W09-000-370). Lane 5: A431 Lysate (p/n W09-000-361). Lane 6: A549 Lysate (p/n W09-001-372). Lane 7: LNCap Lysate (p/n W09-001-GJ9). Lane 8: MOLT-4 Lysate (p/n W09-001-GK2). Lane 9: Ramos Lysate (p/n W09-000-GK4). Lane 10: Raji Lysate (p/n W09-001-368). Lane 11: A-172 Lysate (p/n W09-001-GL5). Lane 12: NIH/3T3 Lysate (p/n W10-000-358). Load: 10 µg per lane. Primary antibody: SMAD3 pS423 pS425antibody at 1ug/mL overnight at 4C. Secondary antibody: Peroxidase rabbit secondary antibody (p/n 611-103-122) at 1:30,000 for 60 min at RT. Blocking Buffer: 1% Casein-TTBS (p/n MB-082) for 30 min at RT. Predicted/Observed size: 35 kDa for SMAD3 pS423 pS425.

References

- Sasaki SI et al. Lacking TRPA1 cation channel impairs primary closure of a stromal incision injury in a mouse cornea. *Lab Invest.* (2025)
- Li JSF et al. Protocol to study immunodynamics in the tumor microenvironment using a tyramide signal amplification-based immunofluorescent multiplex panel. *STAR Protoc.* (2024)
- Yuan Y et al. Targeted PLK1 suppression through RNA interference mediated by high-fidelity Cas13d mitigates osteosarcoma progression via TGF-β/Smad3 signalling. *J Cell Mol Med.* (2024)
- Tartaglia G et al. Antiviral drugs prolong survival in murine recessive dystrophic epidermolysis bullosa. *EMBO Mol Med.* (2024)
- Li JC et al. Angiotensin II mediates hypertensive cardiac fibrosis via an Erbb4-IR-dependent mechanism. *Mol Ther Nucleic Acids.* (2023)
- Chung JYF et al. Smad3 is essential for polarization of tumor-associated neutrophils in non-small cell lung carcinoma. *Nat Commun.* (2023)
- Cao Q et al. Collagen VII maintains proteostasis in dermal fibroblasts by scaffolding TANGO1 cargo. *Matrix Biol.* (2022)
- El-Gazzar, A et al. SMAD3 mutation in LDS3 causes bone fragility by impairing the TGF-β pathway and enhancing osteoclastogenesis. *Bone Reports* (2022)
- Yao L et al. Temporal control of PDGFRα regulates the fibroblast-to-myofibroblast transition in wound healing. *Cell Rep.* (2022)
- Iida R et al. Deficiency of M-LP/Mpv17L leads to development of β-cell hyperplasia and improved glucose tolerance via activation of the Wnt and TGF-β pathways. *Biochim Biophys Acta Mol Basis Dis.* (2022)

- Wang W et al. SARS-CoV-2 N Protein Induces Acute Kidney Injury via Smad3-Dependent G1 Cell Cycle Arrest Mechanism. *Adv Sci (Weinh).* (2022)
- Tang PCT et al. Smad3 Promotes Cancer-Associated Fibroblasts Generation via Macrophage–Myofibroblast Transition. *Adv Sci (Weinh).* (2022)
- Pinkaew D et al. Fortilin interacts with TGF-β1 and prevents TGF-β receptor activation. *Commun Biol.* (2022)
- Yoshimoto Y et al. Tenogenic Induction From Induced Pluripotent Stem Cells Unveils the Trajectory Towards Tenocyte Differentiation. *Front Cell dev Biol.* (2022)
- Tamura Y et al. Anti-pyroptotic function of TGF-β is suppressed by a synthetic dsRNA analogue in triple negative breast cancer cells. *Mol Oncol.* (2021)
- Dong L et al. Deletion of Smad3 protects against diabetic myocardiopathy in db/db mice. *J Cell Mol Med.* (2021)
- Bosch-Queralt M et al. Diet-dependent regulation of TGFβ impairs reparative innate immune responses after demyelination. *Nat Metab.* (2021)
- Takagaki Y et al. Endothelial autophagy deficiency induces IL6-dependent endothelial mesenchymal transition and organ fibrosis. *Autophagy.* (2020)
- Hutchinson LD et al. Salt-inducible kinases (SIKs) regulate TGFβ-mediated transcriptional and apoptotic responses. *Cell Death Dis.* (2020)
- Kang H et al. Somatic SMAD3-activating mutations cause melorheostosis by up-regulating the TGF-β/SMAD pathway. *J Exp Med.* (2020)
- Navarro R et al. TGF-β-induced IGFBP-3 is a key paracrine factor from activated pericytes that promotes colorectal cancer cell migration and invasion. *Mol Oncol.* (2020)
- Ni J et al. Dual deficiency of angiotensin-converting enzyme-2 and Mas receptor enhances angiotensin II-induced hypertension and hypertensive nephropathy. *J Cell Mol Med.* (2020)
- Kim IY et al. Deletion of Akt1 Promotes Kidney Fibrosis in a Murine Model of Unilateral Ureteral Obstruction. *Biomed Res Int.* (2020)
- Yang F et al. Inhibition of dipeptidyl peptidase-4 accelerates epithelial–mesenchymal transition and breast cancer metastasis via the CXCL12/CXCR4/mTOR axis. *Cancer Res.* (2019)
- Gao R et al. βklotho is essential for the anti-endothelial mesenchymal transition effects of N-acetyl-seryl-aspartyl-lysyl-proline. *FEBS Open Bio.* (2019)
- Wei X et al. Spatially restricted stromal Wnt signaling restrains prostate epithelial progenitor growth through direct and indirect mechanisms. *Cell Stem Cell.* (2019)
- Stappenbeck F et al. Inhibition of Non-Small Cell Lung Cancer Cells by Oxy210, an Oxysterol-Derivative that Antagonizes TGFβ and Hedgehog Signaling. *Cells.* (2019)
- Feng et al. TGF-β Mediates Renal Fibrosis via the Smad3-Erbb4-IR Long Noncoding RNA Axis. *Molecular Therapy* (2018)
- Li et al. Fatty acid receptor modulator PBI-4050 inhibits kidney fibrosis and improves glycemic control. *JCI Insight* (2018)
- Tang et al. Generation of Smurf2 Conditional Knockout Mice. *International Journal of Biological Sciences* (2018)

- Chung et al. TGF-β promotes fibrosis after severe acute kidney injury by enhancing renal macrophage infiltration. *JCI Insight* (2018)
- Huang H et al. Lethal (3) malignant brain tumor-like 2 (L3MBTL2) protein protects against kidney injury by inhibiting the DNA damage–p53–apoptosis pathway in renal tubular cells. *Kidney Int.* (2018)
- Liu L et al. Neuronal transforming growth factor beta signaling via SMAD3 contributes to pain in animal models of chronic pancreatitis. *Gastroenterology.* (2018)
- View More ...

Disclaimer